HHS Public Access

Author manuscript

Biochem Biophys Res Commun. Author manuscript; available in PMC 2017 September 16.

Published in final edited form as:

Biochem Biophys Res Commun. 2016 September 16; 478(2): 546–552. doi:10.1016/j.bbrc.2016.07.096.

Sortilin facilitates VLDL-B100 secretion by insulin sensitive McArdle RH7777 cells

Robert P. Sparks[a], **Wayne C. Guida**[d], **Mark P. Sowden**[b], **Jermaine L. Jenkins**[c], **Matthew L. Starr**[a], **Rutilio A. Fratti**[a], **Charles E. Sparks**[e], and **Janet D. Sparks**[e,*]

[a]School of Molecular and Cellular Biology, Department of Biochemistry, University of Illinois Urbana-Champaign, Urbana, IL 61801

[b]Cardiovascular Research Institute, University of Rochester Medical Center, Rochester, NY 14642

[c]Department of Biochemistry and Biophysics, University of Rochester Medical Center, Rochester, NY 14642

[d]Department of Chemistry, University of South Florida, Tampa, FL 33520

[e]Department of Pathology and Laboratory Medicine, University of Rochester Medical Center, Rochester, NY 14642

Abstract

Studies examining the relationship between cellular sortilin and VLDL-B100 secretion demonstrate inconsistent results. Current studies explore the possibility that discrepancies may be related to insulin sensitivity. McArdle RH7777 cells (McA cells) cultured under serum enriched conditions lose sensitivity to insulin. Following incubation in serum-free DMEM containing 1% BSA, McA cells become insulin responsive and demonstrate reduced apo B secretion. Current studies indicate that insulin sensitive McA cells express lower cellular sortilin that corresponds with reduction in VLDL-B100 secretion without changes in mRNA of either sortilin or apo B. When sortilin expression is further reduced by siRNA knockdown (KD), there are additional decreases in VLDL-B100 secretion. A crystal structure of human sortilin (hsortilin) identifies two binding sites on the luminal domain for the N- and C-termini of neurotensin (NT). A small organic compound (cpd984) was identified that has strong theoretical binding to the N-terminal site. Both cpd984 and NT bind hsortilin by surface plasmon resonance. In incubations with insulin sensitive McA cells, cpd984 was shown to enhance VLDL-B100 secretion at each level of sortilin KD suggesting cpd984 acted through sortilin in mediating its effect. Current results support a role for sortilin to facilitate VLDL-B100 secretion which is limited to insulin sensitive McA cells. Inconsistent reports of the relationship between VLDL-B100 secretion and sortilin in previous

*Corresponding author: Department of Pathology and Laboratory Medicine. University of Rochester School of Medicine and Dentistry, Box 626, 601 Elmwood Avenue, Rochester, New York 14642 United States of America. Phone: 585-275-7755. Fax: 585-756-5337 Janet_Sparks@urmc.rochester.edu.

studies may relate to differing functions of sortilin in VLDL-B100 secretion depending upon insulin sensitivity.

Keywords

apo B; sortilin; VLDL-B100; liver; neurotensin; surface plasmon resonance

1. Introduction

The role of sortilin in VLDL-B100 secretion is controversial [1], and inconsistencies have been summarized [2, 3]. Some studies suggest sortilin serves as a chaperone where sortilin is hypothesized to facilitate secretion of VLDL-B100 [4]. Other studies demonstrate that sortilin inhibits VLDL-B100 secretion by trafficking towards degradation [5]. An obligatory inverse relationship is hypothesized to result in VLDL-B100 hypersecretion when sortilin is reduced under conditions of severe insulin resistance [6]. Understanding sortilin function is important considering that sortilin is involved in LDL metabolism [7], and is associated with cardiovascular disease [8]. Studies using surface plasmon resonance (SPR) indicate that human VLDL and LDL, both B100-containing lipoproteins, bind to sortilin [4, 5]. We directly demonstrated enhanced binding of B100 to sortilin with insulin in insulin responsive McArdle RH7777 (McA) cells [9] suggesting the importance of insulin sensitivity in B100 sortilin interaction. Accordingly, the observed inconsistencies in the relationship between sortilin and VLDL-B100 secretion may relate to insulin sensitivity. Culture conditions of McA cells are known to affect insulin signaling and VLDL secretion, and under serum-enriched conditions McA cells are insulin resistant [10]. Using this model we have explored the relationship of cellular sortilin and VLDL-B100 secretion in insulin sensitive McA cells. Under these defined conditions, we show a role for sortilin in facilitating VLDL-B100 secretion. In contrast, in insulin resistant McA cells, VLDL-B100 is secretion is relatively independent of sortilin. Results demonstrate the complexity of sortilin function and the importance of defining metabolic conditions when examining sortilin and VLDL-B100 relationships.

2. Materials and methods

2.1. Cell culture, materials and reagents

McArdle RH-7777 cells (McA cells) were cultured as previously described in serum containing complete Dulbecco's Modified Eagle's Medium (cDMEM) [9, 10]. To induce insulin sensitivity, McA cells at 50-60% confluency were incubated for 18 h in serum-free media consisting of DMEM containing 1% (w/v) BSA (1% BSA/DMEM). Human sortilin (hsortilin) (Ser78-Asn755) with C-terminal 6-His tag was from R&D Systems, Inc., (Minneapolis, MN). Plasma from fasted Sprague Dawley rats (BioreclamationIVT, Westbury, NY) was used to prepare VLDL apo B standards. Mouse monoclonal antibody to rat B100 was prepared in our laboratory and characterized previously [11]. Rabbit anti-sortilin antibody was from GeneTex (GTX54854, Irvine, CA) or from Abcam (ab16640, Cambridge, MA). Rabbit anti-*p*-AKT (9271), rabbit anti-AKT (9272), and rabbit anti-insulin receptor β-subunit (IRβ, 3025) were from Cell Signaling Technology (Danvers, MA). Mouse

anti-*p*Y Platinum 4G10 was from EMD Millipore (Temecula, CA). (Horseradish peroxidase linked donkey anti-rabbit IgG (NA9340), sheep anti-mouse IgG (NXA931) and ECL Prime Western Blotting Detection Reagent (RPN2232) were from GE Healthcare (Buckinghamshire, UK). All other materials and reagents were essentially as described previously [9]. Compound 98477898 (2S)-1-methyl-N-{3-[(3-phenylpropanoyl)-amino]phenyl}pyrrolidine-2-carboxamide (cpd984) was obtained from ChemBridge Corp. (San Diego, CA). A stock solution of cpd984 (10 mM) was prepared in DMSO, and stored in aliquots at −20 °C.

2.2. Knockdown of sortilin in McArdle cells using siRNA

McA cells were transfected using Fugene6 according to manufacturer's protocol (Promega Corp., Madison WI) using three different pGIPZ based vectors expressing shRNAi targeting rat *Sort1* mRNA (V2LMM_58553, V3LMM_450660, V3LMM_450662), and one scrambled, non-silencing control (GE Healthcare Dharmacon, Lafayette, CO). McA cells with sortilin knockdown (KD) were selected using puromycin. Lysates from each cell line were examined by immunoblotting to assess sortilin expression relative to the non-silencing control cells (SCR).

2.3. Immunoblotting

McA cell lysates were prepared and denatured proteins were separated by SDS-PAGE as described previously [10]. Following electrophoretic transfer to PVDF membranes and blocking non-specific binding, membranes were incubated with primary antibodies overnight at 4 ºC in blocking buffer. Antibody binding was detected by incubation for 1-2 h at room temperature with species specific secondary HRP-linked antibodies and developed using Amersham™ Prime reagent (GE Healthcare). Insulin signaling to IRβ and AKT were evaluated using nitrocellulose membranes (Bio-Rad) and phosphospecific (*p*Y, *p*-AKT(Ser473) and mass specific antibodies [12]. Chemiluminescence was measured using the ChemiDocXRS+ system (Bio-Rad) and band intensities quantified using Image Lab 3.0.1 software (Bio-Rad).

2.4. RNA isolation and mRNA quantitation

Total RNA was extracted using TriZol Reagent (Life Technologies, Grand Island, NY) and mRNA was measured by quantitative polymerase chain reaction after reverse transcription as previously described [10] by the University of Rochester Genomic Research Center. TaqMan® gene expression primer probe sets used for fluorogenic quantification of rat mRNA transcripts were: *apoB*, Rn01499054; *Sort1*, Rn01521847, *Atf3*, Rn00563784 and *Rplp0* (ARBP, 36B4), Rn00821065.

2.5. Immuno slot blotting

Experimental media were adjusted to 1% (v/v) protease inhibitor cocktail I (EMD Millipore) and to a salt density of 1.019 g/ml by addition of a solution of NaBr (d = 1.495 g/ml). VLDL was isolated by ultracentrifugation in a L-70 Ultracentrifuge (Beckman Coulter, Inc., Fullterton, CA) using a 50Ti rotor (200,000 x g, 18 h, 14 °C). Following centrifugation, the top 1.5 – 2.0 ml VLDL fraction was removed using a syringe and weighed to determine

volume. VLDL samples were applied in triplicate wells (0.2 to 0.4 ml per well) in a Bio-Dot® SF apparatus (Bio-Rad). Two PVDF membranes were used together for blotting: the top was Immobilon-P (IPVH09120 SF) and the bottom was Immobilin-P^{SQ} (ISEQ09120 SF); both were obtained from EMD Millipore. VLDL apo B standards were prepared from rat plasma VLDL and total apo B (B100 and B48) and B100 content were determined on stained gels following SDS-PAGE separation [13]. VLDL-apo B standards in TBS were slotted in duplicate alongside test samples. After filtration, 0.4 ml of TBS was added as a wash. After final filtration, membranes were air dried, rehydrated in methanol and incubated in TBS then in blocking buffer at 4 ºC overnight. At this stage slot blots were evaluated similarly to immunoblotting. After chemiluminescence development and B100 quantitation, slot blots were stripped by incubation in Restore™ PLUS for 15 min at room temperature (Thermo Scientific, Rockford, IL) and were reblocked overnight at 4 ºC. Total apo B (B100 and B48) present in VLDL was then evaluated following incubation with rabbit polyclonal anti-rat apo B. The bottom PVDF membrane was carried through the entire procedure to assure there was no “bleed through” of test samples. VLDL-apo B and VLDL-B100 content were calculated from standard curves generated by VLDL apo B standards. Recovery of rat VLDL added to unspent media averaged 94% ± 4.9% with a CV of 5.2% (n = 6 replicates).

2.6. Surface Plasmon Resonance

Surface plasmon resonance measurements were performed on a Biacore T200 instrument equipped with Ni-NTA sensor chips with ~6800 response units (RU) for hsortilin covalently immobilized to the surface. HBS-DMSO running buffer (10 mM Hepes pH 7.4, 150 mM NaCl, 1% DMSO) was used at a flow rate of 30 μl/min and injections performed with times for association of 90 sec, and dissociation of 300 sec, followed by injection of buffer to regenerate the hsortilin surface. Binding was expressed in relative RU; the difference in response between the immobilized protein flow cell and the corresponding control flow cell. NT was administered to the chip containing hsortilin at a concentration of 100 nM. NT at the same concentration of 100 nM was then administered in the presence of cpd984.

2.7. Computational modeling and compound screening

Schrödinger’s Maestro program (version 9.3.5) was used as the primary graphical user interface and Maestro version 10.2 (Schrödinger, LLC, New York, NY) was used for ligand interaction diagramming. Virtual screening was performed on compounds contained in ChemBridge libraries (www.chembridge.com) that were prepared with Schrödinger’s LigPrep program [14]. The virtual screening method was performed using Schrödinger’s GLIDE software [15] on the hsortilin crystal structure PDB ID: 4PO7 [16]. Compounds were docked using GLIDE at the site where the N-terminal fragment of NT is found in the crystal structure and cpd984 was chosen for biological screening based on its docking score. Schrödinger’s PRIME software was used to generate missing side chains and loops of this crystal structure predicting the NT peptide spanning the cavity of hsortilin [17]. LigPrep was used on the N-terminal peptide XLYEN-OH from this crystal structure and it was then docked back into its respective site on the crystal structure. This self-docking task was able to reproduce the X-ray pose for this ligand.

2.8. Statistics

Unless noted, results are expressed as the mean ± S.E.M., where n equals the number of independent experiments in which replicate analyses were performed in each experiment. Significant differences were assessed using Student's *t*-test with p-values ≤ 0.05 being considered significant.

3. Results and discussion

3.1. Reduced sortilin levels associate with lower VLDL apo B secretion

We have reported different levels of media accumulation of apo B by McA cells based on culture conditions [10]. Under serum enriched conditions (cDMEM), McA cells are insensitive to insulin activation of Class IA phosphatidylinositide 3-kinase (PI3K); insulin dependent translocation of activated PI3K to intracellular membranes, and fail to express insulin dependent apo B degradation (IDAD) [10]. However, following 18 h incubations in 1% BSA/DMEM, insulin sensitivity is restored while total medium apo B concentration is reduced [10]. We extended these results to measurement of VLDL apo B, and specifically to VLDL-B100, the major form of apo B secreted by McA cells [18], and the only form secreted by human liver. Using these conditions, we addressed the extent to which VLDL-apo B secretion was altered (Fig. 1A). Media VLDL-B100 was analyzed by immuno slot blotting following isolation by ultracentrifugation at d < 1.019 g/ml (Fig. 1B). Consistent with our previous report, both VLDL-apo B total and VLDL-B100 secretion were significantly reduced in insulin sensitive compared with insulin insensitive McA cells. Secreted VLDL-apo B total (ng/mg/18 h) averaged (mean ± SD, n = 5): 1595 ± 40 in cDMEM *vs* 1142 ± 79 in cDMEM. Secreted VLDL-B100 (ng/mg/18h) averaged (mean ± SD, n = 5): 1245 ± 208 *vs* 894 ± 95 in 1% BSA/DMEM. Reduced VLDL secretion was not due to deficiency in fatty acid availability as lipid-enriched BSA was used in the 1% BSA/DMEM medium. Following 1% BSA/DMEM incubation, cellular sortilin levels were significantly depressed (Fig. 1C) averaging only 37% ± 7% (n = 4, p < 0.001) of that present in cells incubated in cDMEM. Reduced apo B secretion and cellular sortilin were not the consequence of lowered abundance of mRNA transcripts as *Apob* and *Sort1* mRNA levels were unchanged by culture conditions (Fig. 1D). Considering the suggested role for transcriptional repression of sortilin by the endoplasmic reticulum stress target ATF3 [6], we also measured *Atf3* mRNA levels. *Atf3* mRNA was reduced on average by 30% in insulin sensitive compared with insensitive McA cells. Decreased ATF3 would be expected to correlate with increased cellular sortilin if there were transcriptional suppression. A corresponding reduction in VLDL-B100 secretion with reduced cellular sortilin suggests a direct relationship. Results are consistent with a model of genetic deletion of sortilin where VLDL-B100 secretion is also reduced [4].

3.2. Sortilin KD in insulin sensitive McA cells associates with decreased VLDL-B100 secretion

If reduced VLDL-B100 secretion were related to lower cellular sortilin, we would expect that additional reductions of sortilin would suppress VLDL-B100 even further. To address this premise, we prepared three stable cell lines of McA cells using siRNA with variable KD of sortilin compared with wildtype (WT) and McA cells transfected with scrambled shRNA

(SCR)(Fig. 2A). The low (L), medium (M) and high (H) sortilin expressing McA cell lines were incubated in cDMEM, and VLDL-B100 secretion was measured (Fig. 2B). There was no reduction in VLDL-B100 secretion observed with progressively reduced sortilin. There was a small but significant increase in VLDL-B100 secretion in the lowest sortilin expressing McA53 cells (L) compared with SCR that averaged 32% ($p < 0.05$). In contrast, in each McA cell line incubated in 1% BSA/DMEM, there was reduced VLDL-B100 secretion (Fig. 2C). Alterations in the relationship between VLDL-B100 secretion and sortilin under differing culture conditions suggest differences in sortilin function with insulin sensitivity.

3.3. Identification of a small molecule that binds the N-terminal NT binding site on hsortilin

The complexity of sortilin function as a multi-ligand receptor may be related to different sites of ligand binding which direct different functions of sortilin. High resolution crystal structures of hsortilin have been reported, and a C-terminal NT binding site forming a salt bridge between the C-terminal carboxylate of NT and arginine 292 (R292) of the crystal structure have been identified (Fig. 3A) [16]. Small molecules that bind to this site have been characterized [19]. The N-terminus of NT (pyroGlu-Leu-Tyr-Glu-Asn) also interacts with hsortilin [16]. Using Schrödinger software, we explored the N-terminal NT binding site screening compounds from the ChemBridge library and further characterized NT fragments present in the hsortilin crystal structure PDB ID: 4PO7 (Fig. 3A) [16]. We identified cpd984 which had a high predicted affinity to the N-terminal NT binding site using GLIDE XP [15] with a gscore of −9.0 kcal/mol binding strength as compared with a gscore of −8.9 kcal/mol for the N-terminal NT sequence. The position of cpd984 relative to critical amino acid residues of this region is shown (Fig. 3B). Surface amino acids at the binding site for N-terminal NT correspond with amino acids in the interaction diagram presented for cpd984 indicating similar regions of binding.

3.4. Cpd984 and NT bind to hsortilin

To confirm that cpd984 was bound by hsortilin at a NT-related binding site, we performed SPR (Fig. 3C). We show that individually NT (red, lower curve) and cpd984 (green, middle curve) bind hsortilin. The presence of cpd984 resulted in an increase of 14.5 RU for co-injected NT (black, upper curve) over the RU of the combination of NT and 984 alone. Considering the larger size of NT, the increase in RU likely represents enhancement of NT binding to hsortilin by cpd984.

3.5. Cpd984 increases VLDL-B100 secretion by insulin sensitive McA cell

We next tested whether cpd984 alters sortilin function in insulin sensitive McA cells (Fig. 3D). Cpd984 increased VLDL-B100 secretion with significant increases observed at 10 μM and 25 μM averaging 30% and 61%, respectively, over control.

3.6 Cpd984 increases VLDL-B100 secretion by McA cells under-expressing sortilin

To evaluate the effect of cpd984 on sortilin deficient McA cells, McA cell lines with sortilin KD were incubated with 10 μM cpd984. Cpd984 significantly enhanced VLDL-B100 secretion in each cell line (Fig. 4B). Incubation of McA cells with cpd984 did not alter

insulin sensitivity, as insulin-dependent *p*Y of IRβ and stimulation of *p*AKT(S473) were not affected (Fig. 4C). Reduced VLDL-B100 secretion occurred in both M (McA62) and L (McA53) cell lines with and without cpd 984 added ($p < 0.05$). Although the mechanism of action of cpd984 is not fully established, its action is likely mediated through interaction with sortilin as although VLDL-B100 secretion is increased, it is still lower with reduced sortilin suggesting sortilin remains rate-limiting.

The complex relationship between sortilin and VLDL-B100 secretion is demonstrated in the current study. We show a rate-limiting role for sortilin in VLDL-B100 secretion that is present only in insulin sensitive McA cells and correlates with sortilin expression. Previous studies have shown that binding of B100 to sortilin is enhanced by insulin [9], and precedes B100 degradation mediated by autophagy [12]. With insulin sensitivity, apo B mRNA is unchanged so the decrease in VLDL-B100 secretion observed in 1% BSA/DMEM is likely due to baseline degradation. Together, these data suggest that baseline B100 degradation is further enhanced by insulin which reverses the role of sortilin as a secretory chaperone and directs B100 to autophagy, a pathway seen only with insulin sensitivity. A reasonable explanation for divergent effects of sortilin on VLDL-B100 secretion is the presence of multiple binding sites on sortilin that with binding result in different functions. We speculate that cpd984 may occupy a site on sortilin that enhances VLDL-B100 secretion through the N terminal NT binding domain that favors the chaperone function of sortilin. Further studies will be necessary to define binding sites and functional relationships. Results presented in this study demonstrate that there is not an obligatory reciprocal relationship between sortilin expression and VLDL B100 secretion, and that the function of sortilin in McA cells depends on insulin sensitivity. Resolution of the controversies related to sortilin and VLDL-B100 secretion may be facilitated by identification of small molecules that bind different sites on sortilin and promote different sortilin function.

Supplementary Material

Refer to Web version on PubMed Central for supplementary material.

Acknowledgements

This study was supported by grants from the National Institutes of Health DK100163 (JDS) and GM101132 (RAF).

Abbreviations

Apo B	apolipoprotein B
B100	apo B derived from unedited *Apob* mRNA
IDAD	insulin dependent apolipoprotein B degradation
McA	McArdle RH7777 cells
PI3K	Class IA phosphatidylinositide 3-kinase
SPR	surface plasmon resonance

VLDL very low density lipoprotein

References

[1]. Sparks CE, Sparks RP, Sparks JD. The enigmatic role of sortilin in lipoprotein metabolism. Curr. Opin. Lipidol. 26(2015):598–600. [PubMed: 26780014]

[2]. Strong A, Patel K, Rader DJ. Sortilin and lipoprotein metabolism: making sense out of complexity. Curr. Opin. Lipidol. 25(2014):350–357. [PubMed: 25101658]

[3]. Kjolby M, Nielsen MS, Petersen CM. Sortilin, encoded by the cardiovascular risk gene SORT1, and its suggested functions in cardiovascular disease. Curr. Atheroscler. Rep. 2015; 17:496. [PubMed: 25702058]

[4]. Kjolby M, Andersen OM, Breiderhoff T, Fjorback AW, Pedersen KM, Madsen P, Jansen P, Heeren J, Willnow TE, Nykjaer A. Sort1, encoded by the cardiovascular risk locus 1p13.3, is a regulator of hepatic lipoprotein export. Cell Metab. 12(2010):213–223. [PubMed: 20816088]

[5]. Strong A, Ding Q, Edmondson AC, Millar JS, Sachs KV, Li X, Kumaravel A, Wang MY, Ai D, Guo L, Alexander ET, Nguyen D, Lund-Katz S, Phillips MC, Morales CR, Tall AR, Kathiresan S, Fisher EA, Musunuru K, Rader DJ. Hepatic sortilin regulates both apolipoprotein B secretion and LDL catabolism. J. Clin. Invest. 122(2012):2807–2816. [PubMed: 22751103]

[6]. Ai D, Baez JM, Jiang H, Conlon DM, Hernandez-Ono A, Frank-Kamenetsky M, Milstein S, Fitzgerald K, Murphy AJ, Woo CW, Strong A, Ginsberg HN, Tabas I, Rader DJ, Tall AR. Activation of ER stress and mTORC1 suppresses hepatic sortilin-1 levels in obese mice. J. Clin. Invest. 122(2012):1677–1687. [PubMed: 22466652]

[7]. Patel KM, Strong A, Tohyama J, Jin X, Morales CR, Billheimer J, Millar J, Kruth H, Rader DJ. Macrophage sortilin promotes LDL uptake, foam cell formation, and atherosclerosis. Circ. Res. 116(2015):789–796. [PubMed: 25593281]

[8]. Musunuru K, Strong A, Frank-Kamenetsky M, Lee NE, Ahfeldt T, Sachs KV, Li X, Li H, Kuperwasser N, Ruda VM, Pirruccello JP, Muchmore B, Prokunina-Olsson L, Hall JL, Schadt EE, Morales CR, Lund-Katz S, Phillips MC, Wong J, Cantley W, Racie T, Ejebe KG, Orho-Melander M, Melander O, Kotelianski V, Fitzgerald K, Krauss RM, Cowan CA, Kathiresan S, Rader DJ. From noncoding variant to phenotype via SORT1 at the 1p13 cholesterol locus. Nature. 466(2010):714–719. [PubMed: 20686566]

[9]. Chamberlain JM, O'Dell C, Sparks CE, Sparks JD. Insulin suppression of apolipoprotein B in McArdle RH7777 cells involves increased sortilin 1 interaction and lysosomal targeting. Biochem. Biophys. Res. Commun. 430(2013):66–71. [PubMed: 23159624]

[10]. Sparks JD, Magra AL, Chamberlain JM, O'Dell C, Sparks CE. Insulin dependent apolipoprotein B degradation and phosphatidylinositide 3-kinase activation with microsomal translocation are restored in McArdle RH7777 cells following serum deprivation. Biochem. Biophys. Res. Commun. 469(2016):326–331. [PubMed: 26616056]

[11]. Sparks JD, Bolognino M, Trax PA, Sparks CE. The production and utility of monoclonal antibodies to rat apolipoprotein B lipoproteins. Atherosclerosis. 61(1986):205–211. [PubMed: 2429674]

[12]. Sparks JD, O'Dell C, Chamberlain JM, Sparks CE. Insulin-dependent apolipoprotein B degradation is mediated by autophagy and involves class I and class III phosphatidylinositide 3-kinases. Biochem. Biophys. Res. Commun. 435(2013):616–620. [PubMed: 23685141]

[13]. Chirieac DV, Davidson NO, Sparks CE, Sparks JD. PI3-kinase activity modulates apo B available for hepatic VLDL production in apobec-1−/− mice. Am. J. Physiol. 2006; 291:G382–388.

[14]. 2014 Schrodinger, LigPrep, Schrodinger, Schrodinger, LLC, New York, NY.

[15]. Halgren TA, Murphy RB, Friesner RA, Beard HS, Frye LL, Pollard WT, Banks JL. Glide: a new approach for rapid, accurate docking and scoring. 2. Enrichment factors in database screening. J. Med. Chem. 47(2004):1750–1759. [PubMed: 15027866]

[16]. Quistgaard EM, Groftehauge MK, Madsen P, Pallesen LT, Christensen B, Sorensen ES, Nissen P, Petersen CM, Thirup SS. Revisiting the structure of the Vps10 domain of human sortilin and its interaction with neurotensin. Protein Sci. 23(2014):1291–1300. [PubMed: 24985322]

[17]. Jacobson MP, Pincus DL, Rapp CS, Day TJ, Honig B, Shaw DE, Friesner RA. A hierarchical approach to all-atom protein loop prediction. Proteins. 55(2004):351–367. [PubMed: 15048827]

[18]. Kummrow E, Hussain MM, Pan M, Marsh JB, Fisher EA. Myristic acid increases dense lipoprotein secretion by inhibiting apoB degradation and triglyceride recruitment. J. Lipid Res. 43(2002):2155–2163. [PubMed: 12454278]

[19]. Schroder TJ, Christensen S, Lindberg S, Langgard M, David L, Maltas PJ, Eskildsen J, Jacobsen J, Tagmose L, Simonsen KB, Biilmann Ronn LC, de Jong IE, Malik IJ, Karlsson JJ, Bundgaard C, Egebjerg J, Stavenhagen JB, Strandbygard D, Thirup S, Andersen JL, Uppalanchi S, Pervaram S, Kasturi SP, Eradi P, Sakumudi DR, Watson SP. The identification of AF38469: an orally bioavailable inhibitor of the VPS10P family sorting receptor Sortilin. Bioorg. Med. Chem. Lett. 24(2014):177–180. [PubMed: 24355129]

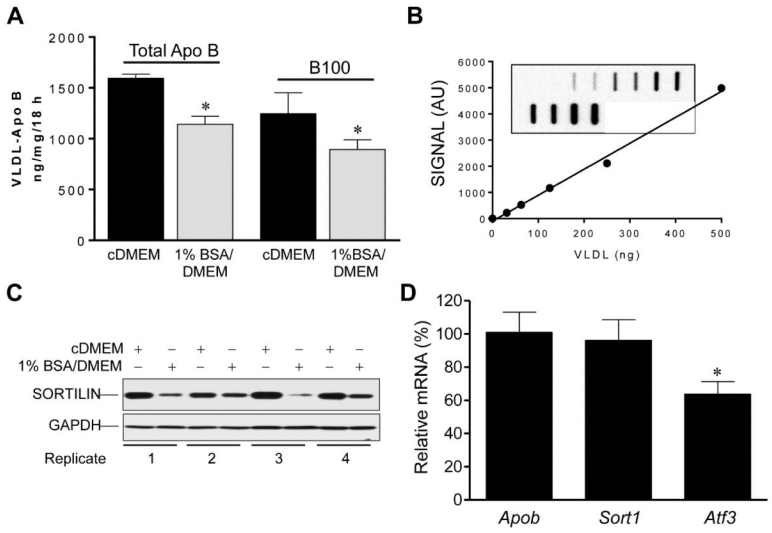

Fig. 1. VLDL-apo B secretion and sortilin expression in McA cells

(A) VLDL-apo B and VLDL-B100 secretion were measured following 18 h incubation of McA cells in cDMEM (black bars) and in 1% BSA/DMEM (gray bars) by immuno slot blotting. (B) Representative standard curve generated from an immuno slot blot (duplicate standards) where VLDL protein is plotted against average chemiluminescence signal in arbitrary units (AU) generated using anti-rat B100 monoclonal antibody and HRP-anti-mouse IgG. (C) Immunoblots of McA cell lysates from four independent experiments comparing McA cells incubated in cDMEM with 1% BSA/DMEM. Anti-GAPDH blotting display equal protein loading. (D) Relative expression of *Apob*, *Sort1* and *Atf3* mRNA in McA cells incubated in 1% BSA/DMEM as a percentage of mRNA present in McA cells incubated in cDMEM. Results are averages from 4 independent experiments.* Indicates means are significantly different.

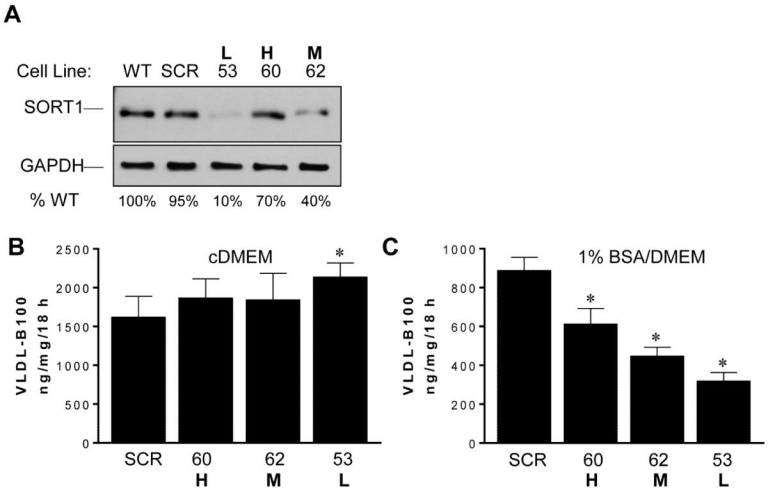

Fig. 2. Effect of variable sortilin expression on secretion of VLDL-B100 by McA cells

(A) Following siRNA-mediated KD of sortilin, three clones of McA cells were selected representing high (H, McA60), medium (M, McA62) and low (L, McA53) sortilin expression evaluated by immunoblotting compared with wild type (WT) McA cells. The effect of increasing sortilin KD on VLDL-B100 secretion by McA cells incubated in cDMEM (B) or incubated in 1% BSA/DMEM (C). Results in (B) and (C) are averages of triplicate plates for each condition (n = 2 studies). * Indicates means are significantly different from the SCR McA cell line.

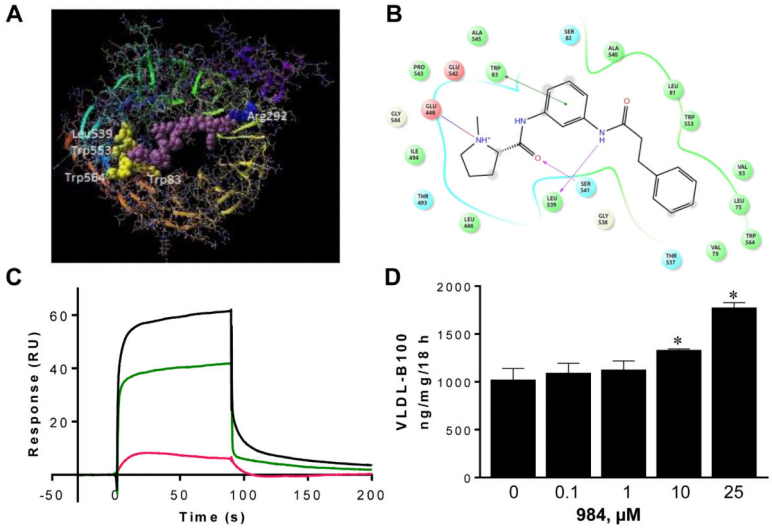

Fig. 3. Binding characteristics of NT and cpd984 to hsortilin

(A) Schrödinger's PRIME was run on PDB ID: 4PO7 predicting missing side chains of NT connecting two fragments of the peptide from the crystal structure across the length of the cavity of hsortilin. The predicted peptide XLYENKPRRPYIL generated by connecting C-terminal fragment PYIL-OH and N-terminal fragment XLYEN-OH matches the amino acid sequence for NT and is the right length to connect exactly the N-terminus fitting into site 2 of hsortilin indicated by four of the residues present in the ligand binding diagram of cpd984 generated from the crystal structure. This is depicted in an atomic space filling model and colored yellow and the C-terminal end fitting into site 1 of hsortilin as indicated by the conserved residue R292 of crystal structure 4PO7 is depicted in blue. (B) Ligand interaction diagram depicting binding of cpd984 to hsortilin using Schrödinger's GLIDE indicating key amino acid residues likely to be involved in binding (blue, basic; red, acidic; green, hydrophobic amino acids). Hydrogen bonds are indicated with purple arrows and pi-stacking are indicated with green arrows. (C) Sensograms showing binding of NT to hsortilin (red, lower curve); cpd984 to hsortilin (green, middle curve) and NT binding in the presence of cpd984 (black, upper curve). The binding response in response units (RU) versus time (sec) was plotted of 100 nM NT injected alone less blank (red 4.5 and 5.5 RU) or with 500 μM cpd984 (blue 64.1 and 64.7 RU) and 500 μM cpd984 alone (green 45.1 and 44.8 RU). Subtracting the averaged RU of NT co-injected with 984 (64.4 RU) from 500 μM cpd984 and 100 nM NT (50.0 RU) results in a 14.5 RU increase in binding to hsortilin. (D) McA cells were incubated in 1% BSA'/DMEM containing increasing concentrations of cpd984 for 18 h, and secreted VLDL-B100 was quantified by immuno slot blotting (n = 2 studies). * Indicates means differ from the no cpd984 condition.

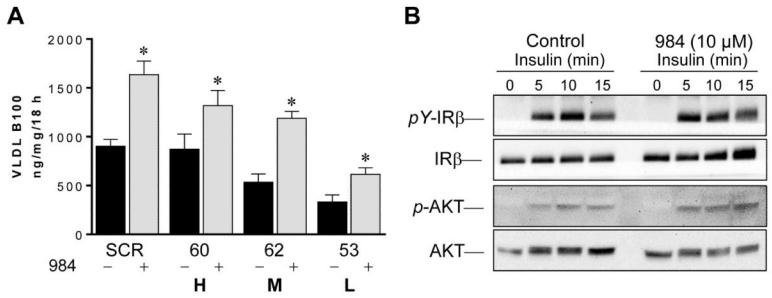

Fig. 4. Effect of cpd984 on VLDL-B100 secretion and on insulin sensitivity in McA cells

(A) McA cell lines with variable sortilin KD were incubated with vehicle (black bars) or with 10 μM cpd984 (gray bars) for 18 h (3-100 mm plates per condition). Viability of McA cells was not compromised by incubations with cpd984 as there was no significant release of LDH into the medium compared with control incubations. VLDL was isolated from media of each plate and VLDL-B100 was quantified by immuno slot blotting. Results presented are averages of the 3 plates ± S.D. (B) McA cells were incubated for 18 h in 1% BSA/DMEM ± 10 μM cpd984. McA cells were then stimulated with a time course of 250 nM insulin (0, 5, 10 and 15 min). IRβ and AKT, *p*Y-IRβ, and *p*-AKT (S473) were evaluated by immunoblotting using protein and phosphospecific antibodies.